How the inclination of Earth's orbit affects incoming solar irradiance

L.E.A. Vieira, A Norton, Thierry Dudok de Wit, Matthieu Kretzschmar, G.A. Schmidt, M.C.M. Cheung

How the inclination of Earth's orbit affects incoming solar irradiance

L. E. A. Vieira,[1] A. Norton,[2] T. Dudok de Wit,[1] M. Kretzschmar,[1,3] G. A. Schmidt,[4] and M. C. M. Cheung[5]

Received 29 June 2012; revised 20 July 2012; accepted 21 July 2012; published 29 August 2012.

[1] The variability in solar irradiance, the main external energy source of the Earth's system, must be critically studied in order to place the effects of human-driven climate change into perspective and allow plausible predictions of the evolution of climate. Accurate measurements of total solar irradiance (TSI) variability by instruments onboard space platforms during the last three solar cycles indicate changes of approximately 0.1% over the sunspot cycle. Physics-based models also suggest variations of the same magnitude on centennial to millennia time-scales. Additionally, long-term changes in Earth's orbit modulate the solar irradiance reaching the top of the atmosphere. Variations of orbital inclination in relation to the Sun's equator could potentially impact incoming solar irradiance as a result of the anisotropy of the distribution of active regions. Due to a lack of quantitative estimates, this effect has never been assessed. Here, we show that although observers with different orbital inclinations experience various levels of irradiance, modulations in TSI are not sufficient to drive observed 100 kyr climate variations. Based on our model we find that, due to orbital inclination alone, the maximum change in the average TSI over timescales of kyrs is $\sim$0.003 Wm^{-2}, much smaller than the $\sim$1.5 Wm^{-2} annually integrated change related to orbital eccentricity variations, or the 1–8 Wm^{-2} variability due to solar magnetic activity. Here, we stress that out-of-ecliptic measurements are needed in order to constrain models for the long-term evolution of TSI and its impact on climate. **Citation:** Vieira, L. E. A., A. Norton, T. Dudok de Wit, M. Kretzschmar, G. A. Schmidt, and M. C. M. Cheung (2012), How the inclination of Earth's orbit affects incoming solar irradiance, *Geophys. Res. Lett.*, *39*, L16104, doi:10.1029/2012GL052950.

1. Introduction

[2] Since the sunspot cycle was discovered, the Sun has been considered as a possible agent of climate change [e.g., *Eddy*, 1976]. However, due to difficulties in distinguishing between solar, volcanic, and anthropogenic influences [*Ammann et al.*, 2003; *Cubasch et al.*, 2001; *Schmidt et al.*, 2012], as well as complex responses related to cloud cover and ocean temperatures [*Hansen*, 2000], its precise role is still subject to controversy. A common measure of the Sun's energy output is Total Solar Irradiance (TSI), defined as the wavelength-integrated flux of radiation received at the top of Earth's atmosphere. The TSI has a baseline value of approximately 1361 Wm^{-2} during minima in solar activity [*Kopp and Lean*, 2011].

[3] Since 1978, TSI variability has been measured with a high accuracy by instruments onboard several space-based platforms. Daily variations up to $\sim$0.3% are caused by the presence of dark (sunspots) and bright (faculae and network) features on the solar surface [*Willson et al.*, 1981]. Intense magnetic fields within sunspots [e.g., *Borrero and Ichimoto*, 2011] suppress convection and reduce the transport of thermal energy from the solar interior to the photosphere. Such a reduction of the surface temperature within sunspots leads to lower surface opacity. Coupled with the fact that sunspots are partially evacuated, relative to the quiet Sun, surfaces of constant optical depth within sunspot umbra are located at deeper geometric depths, the so-called Wilson depression. The energy blocked by sunspots seems to diffuse in the convection zone on short time scales [*Foukal et al.*, 2006] and is stored and released on longer time scales. On the other hand, the structure of the solar magnetic field governs also the leakage of energy that leads to a positive variation of the TSI during the solar cycle. Most magnetic features on the solar surface other than sunspots appear as faculae and network. These are small, bright structures that also block the convection. However, because the flux tubes are narrow, the inflow of radiation through the hot walls exceeds the energy blocked. The geometry of the small-scale fields causes a non-isotropic radiation field [*Spruit*, 1977; *Steiner*, 2005]. The combination of these effects leads to variations in the TSI on time-scales from days, to years (the 11-year sunspot cycle), to millennia [*Shapiro et al.*, 2011; *Steinhilber et al.*, 2009; *Vieira et al.*, 2011].

[4] Previous investigations [*Muller and MacDonald*, 1995] have indicated that the Earth's orbital inclination and climate records present a strong 100 kyr periodicity signal; although no physical mechanism linking the phenomena has been successfully established. Surprisingly, the potential impact of anisotropy on the distribution of active regions on the irradiance variability due to changes in Earth's orbital inclination, on timescales of kyrs, has been overlooked in the literature. Although observational [e.g., *Rast et al.*, 2008] and modeling [e.g., *Knaack et al.*, 2001; *Schatten*, 1993] efforts have been performed in the past, since its observation requires an out-of-ecliptic vantage point, the latitudinal dependence of irradiance

[1]Laboratoire de Physique et Chimie de l'Environnement et de l'Espace, UMR7328, CNRS, University of Orléans, Orléans, France.
[2]HEPL, Solar Physics, Stanford University, Stanford, California, USA.
[3]SIDC, Royal Observatory of Belgium, Brussels, Belgium.
[4]NASA Goddard Institute for Space Studies, New York, New York, USA.
[5]Lockheed Martin Solar and Astrophysics Laboratory, Palo Alto, California, USA.

Corresponding author: L. E. A. Vieira, Laboratoire de Physique et Chimie de l'Environnement et de l'Espace, UMR7328, CNRS, University of Orléans, 3A, Av. de la Recherche, FR-45071 Orléans CEDEX 2, France. (luis.vieira@cnrs-orleans.fr)

0094-8276/12/2012GL052950

is not known. To date, only instruments on spacecraft with near-Earth orbits or at the L1 Lagrangian point have measured the TSI. Unfortunately, missions such as Voyager 2 and Ulysses, which reached high solar latitudes, had no measurements of solar irradiance. The Solar Orbiter Mission has an orbit out of the ecliptic plane and is scheduled to be launched in 2017. However, TSI observations will not be a part of this mission. Therefore, any variability outside the terrestrial vantage point (i.e., outside of the ecliptic plane) has not been sampled and will not be measured in the near future. Since the distribution of solar active regions is limited from mid to low solar latitudes, here we investigate the geometric component of solar irradiance variability that has gone undetected. Specifically, we search for an anisotropy in TSI (flux density) from the solar equator to the poles that could be sampled if the Earth had a highly inclined orbit.

[5] In Section 2 we describe the method employed to compute the out-of-the-ecliptic solar irradiance. Then the modeled evolution of the out-of-the-ecliptic TSI during the ascending phase of cycle 24 is discussed in Section 3. Next, an estimate of TSI variations due to changes in orbital inclination is presented in Section 4. Finally, conclusions are provided in Section 5.

2. Approach

[6] Over the past decade, the TSI has been successfully modeled based on the evolution of the solar surface magnetic field, observed as distinct features [*Ball et al.*, 2012; *Domingo et al.*, 2009; *Krivova et al.*, 2003; *Wenzler et al.*, 2006]. Following *Krivova et al.* [2003] and others, in order to quantitatively reproduce solar irradiance, we segmented the solar disk into the following five features: quiet-Sun (q), sunspot umbrae (u), sunspot penumbra (p), faculae (f), and network (n). Our procedure consists of the feature extraction algorithm and the classification of magnetic concentrations according to the area of the solar surface covered by individual structures. Additionally, we remove magnetic concentrations that individually cover less than 9.1 ppm of the solar disk. The segmented images/synoptic maps were then rotated and mapped onto different points of view in order to reproduce what would be observed from any vantage point at a spherical surface at 1 Astronomical Unit (AU), the average Sun-Earth distance.

[7] Due to projection effects, magnetic field measurements are less accurate near the poles [*Sun et al.*, 2011]. We assume that the greatest variability of the TSI was due to the emergence and decay of large structures between −/+40° of the solar equator (as determined by the butterfly diagram), and that the evolution of very small scale structures, most likely produced by a local surface dynamo [*Vögler and Schüssler*, 2007], are uniformly distributed over the solar surface, including polar regions. Moreover, we suppose that the distribution of very small-scale magnetic concentrations does not change through the 11-year sunspot cycle and that no asymmetries arise from the presence of small scale structures, even if weak fields increase the brightness in the quiet Sun [*Foukal et al.*, 2011; *Schnerr and Spruit*, 2011; *Shapiro et al.*, 2011]. Note that a different spatial distribution of the polar magnetic flux could slightly change the results discussed here. However, our assumption is justified by the fact that we analyze the early part of the ascending phase.

[8] The computed irradiance depends on the area and on the spatial location of features on the solar disk [*Krivova et al.*, 2003]. To determine the distribution of dark and bright magnetic structures on the solar surface, we used the magnetic field and continuum intensity data from the Helioseismic and Magnetic Imager (HMI) [*Schou et al.*, 2012] onboard the Solar Dynamics Observatory (SDO) spacecraft. Spectra computed from models were used to describe the radiative output of the different components of the solar atmosphere [*Unruh et al.*, 1999]. In this manner, the evolution of the radiative flux at a given wavelength, λ, and the given colatitude, θ, could be computed as follows:

$$F(\lambda,\theta,\mu(\theta),t) = \alpha_u(\mu(\theta),t)\Delta F_u(\lambda,\mu(\theta)) + \alpha_p(\mu(\theta),t)\Delta F_p(\lambda,\mu(\theta)) + \alpha_f(\mu(\theta),t)\Delta F_f \cdot(\lambda,\mu(\theta)) + \alpha_n(\mu(\theta),t)\Delta F_n(\lambda,\mu(\theta)) + cF_q(\lambda,\mu(\theta)), \quad (1)$$

where $\mu(\theta)$ is the cosine of the angle between the normal of the solar surface and the observed line-of-sight at the colatitude θ. The functions $\Delta F_u(\lambda,\mu(\theta))$, $\Delta F_p(\lambda,\mu(\theta))$, $\Delta F_f(\lambda,\mu(\theta))$, and $\Delta F_n(\lambda,\mu(\theta))$ are the difference of the time-independent radiative fluxes of the bright and dark components of the model with respect to the quiet-Sun, $cF_q(\lambda,\mu(\theta))$, emergent intensity. Following *Krivova et al.* [2003] and others, we employed the spectrum of each component, $F_i(\lambda,\mu)$, computed by *Unruh et al.* [1999] based on the atmosphere models by *Kurucz* [1993]. Note that in order to match the level of irradiance measured by TIM/SORCE, the quiet sun spectrum is scaled by a factor c = 1.00247, which is an additional free parameter in the model. In this way, the quiet Sun contribution to the TSI in the model is 1360.6 Wm^{-2}. To obtain the spatial distribution of features from the point of view of an observer at different latitudes ($\alpha_i(\mu(\theta),t)$), $i = q,u,p,f,n$), we combined synoptic maps and disk images measured within two hours interval. The filling factors of the individual pixels ($\alpha_{f,\,n}$) of the bright elements were determined by the relationship $\alpha_{f,\,n} = \min(1, B/B_{\mathrm{sat}})$, where B is the magnetic field intensity and B_{sat}, which is a free parameter, is the saturation. Each pixel on the solar surface was then replaced by the corresponding modeled spectrum at the appropriate position on the solar disk. After summing over all pixels, the Sun's irradiance spectrum was obtained and provided a good comparison to the observed irradiance near the ecliptic plane for B_{sat} equal to 104.2 G. The latitudinal profile of the TSI for the central meridian was then computed every 6 hours from a heliographic latitude (with respect to the solar equator), 90°N to 90°S with a latitudinal resolution of 10°. The TSI was calculated for each heliographic latitude, longitude, and time.

3. Out-of-Ecliptic TSI During the Ascending Phase of Cycle 24

[9] Figure 1a shows an example of the modeled temporal evolution of TSI as a function of the heliographic latitude from 19-Jul-2011 to 15-Aug-2011. The time period was chosen to illustrate the effect of three large sunspots in the Northern Hemisphere. Sunspot-induced depletion in total radiative flux density was centered at approximately 30°N with a 120° latitudinal extent that was not symmetric. During this period, the flux at the North Pole is systematically higher

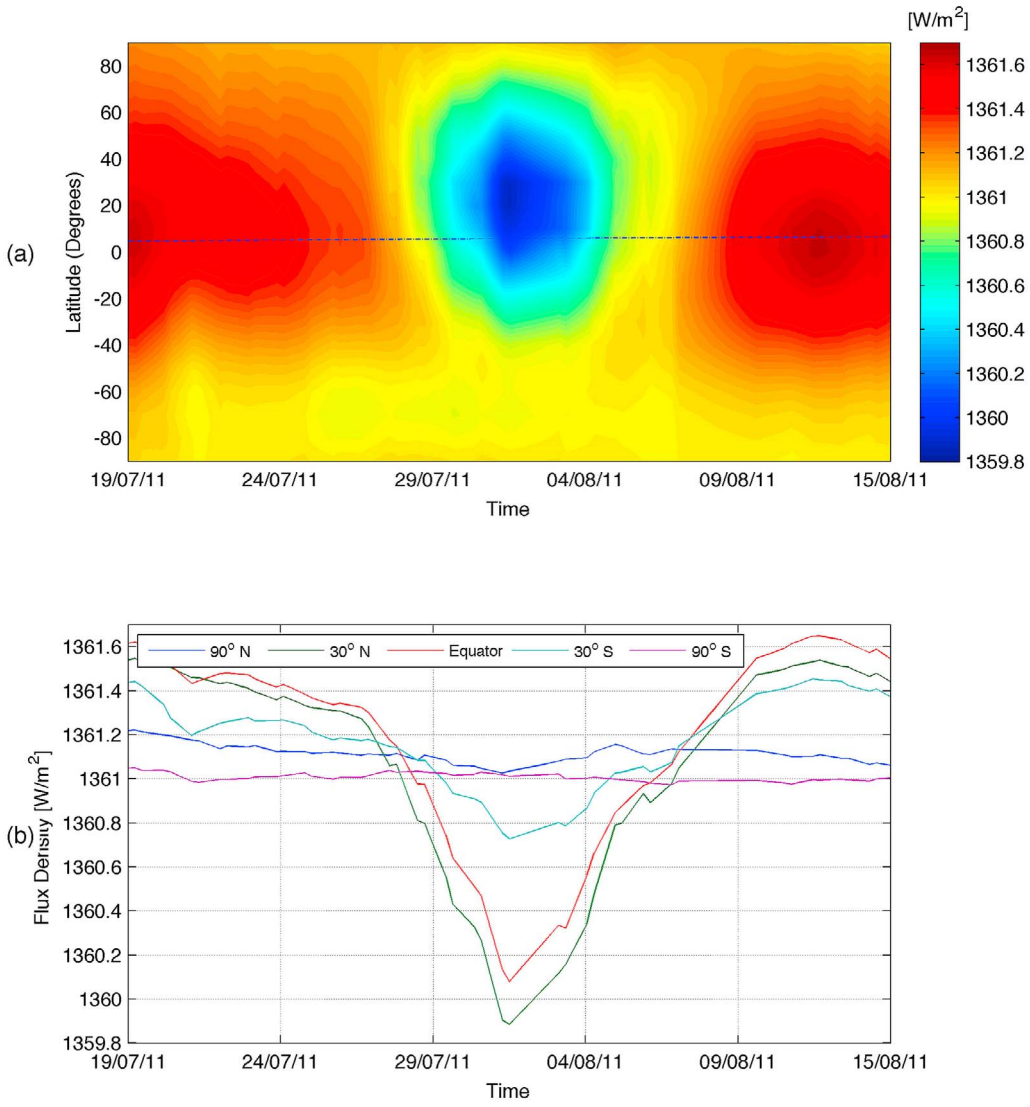

Figure 1. (a) The flux density evolution as a function of latitude for solar features present from 19-Jul-2011 to 15-Aug-2011. During this period, the three sunspot groups are located in the Northern Hemisphere. Above the North Pole of the Sun, an observer would experience an irradiance of 1361.2 W m^{-2}, as compared to 1360.2 W m^{-2} for the Earth's true orbital position, 5.8° North of the solar equator. (b) The temporal evolution flux density from 19-Jul-2011 to 15-Aug-2011 at the latitudes of 90°N, 30°N, equator, 30°S, and 90°S. Individual sunspots are responsible for irradiance decreases that are similar to a short-lived depletion in the radiative flux, not isotropic within the heliosphere.

than in the South Pole due to the imbalance of hemispheric magnetic features. Observers at fixed points of view at 30°N and 30°S would measure a difference of approximately 1 Wm^{-2} near the heliographic longitude of the sunspot groups.

[10] Figure 2a shows the modeled temporal evolution of TSI as a function of the heliographic latitude of the observer. As seen in the Panel (b), the modeled TSI from Earth's vantage point reproduces the observed TSI by TIM/SORCE [*Kopp et al.*, 2005] and VIRGO/SOHO [*Fröhlich et al.*, 1995] instruments extremely well. The TSI experienced by a hypothetical planet or a spacecraft at 1 Astronomical Unit (AU) from the Sun, but with its orbital plane inclined by 30, 45, 60, and 75° with respect to the solar equator, is shown in Panel (c).

[11] The method presented here allows us to address a fundamental question of how solar activity affects the solar luminosity. Changes in the solar luminosity are expected to arise from variations of the solar fusion rate or by the release of energy stored in the radiative and convection zones. If we consider just observations from the Earth's point of view, neither the darkness of sunspots nor the increased flux from the bright component is cancelled by compensating variations in the solar brightness elsewhere on the disk [*Foukal et al.*, 2006]. With our method of modeling the out-of-the-ecliptic flux density, we can estimate the solar luminosity by integrating the flux density for the whole sphere. Figure 2d displays the evolution of the solar luminosity (black line). The blue line shows the power blocked by sunspots, while the red and green lines present the power radiated by large and small-scale bright features, respectively. We consider small-scale structures the ones that individually cover less than 16.4 ppm of the solar disk. The power leaked by small-scale magnetic concentrations increases steadily during the period, while the power radiated by large-scale structures present a larger variability. Two sharp decreases

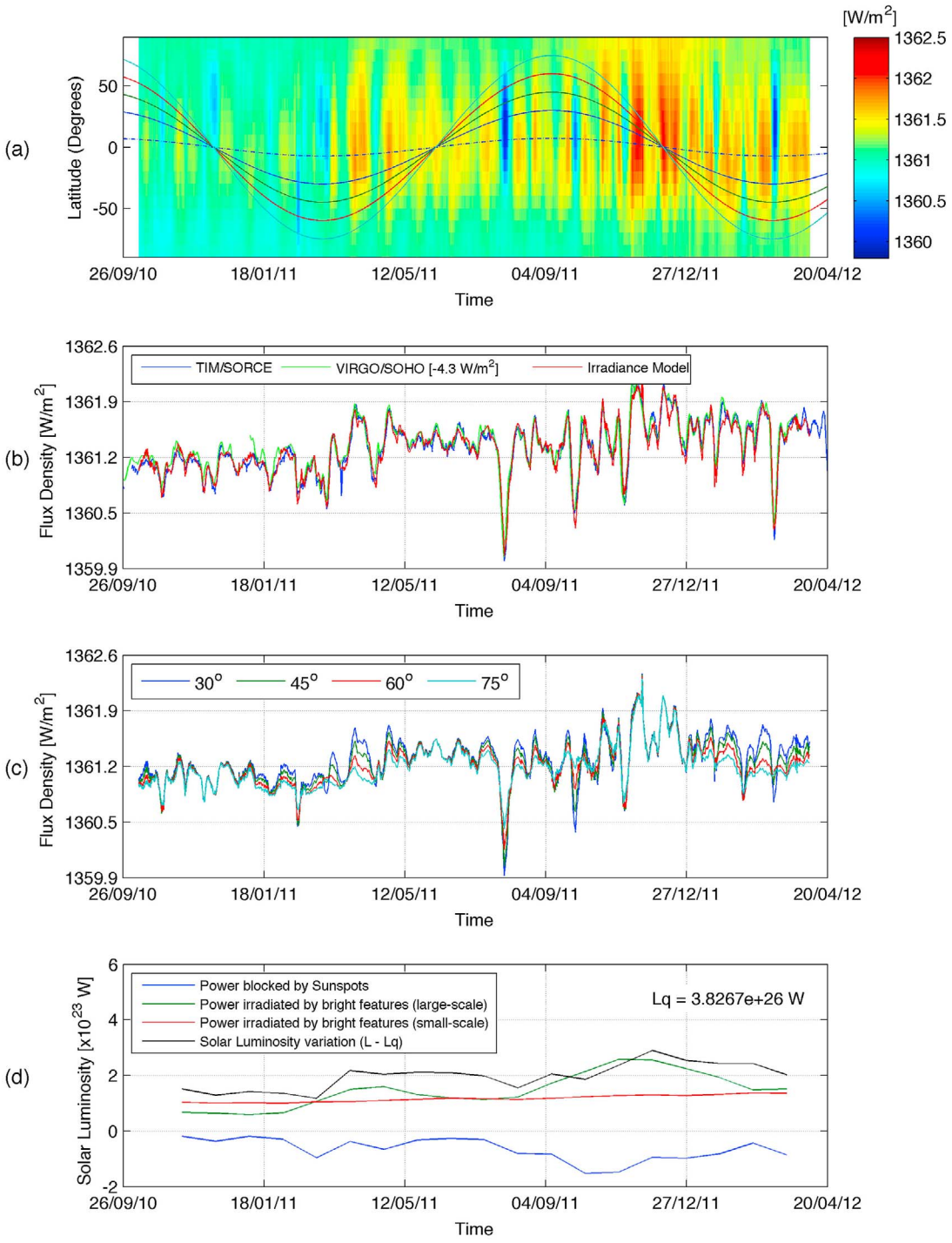

Figure 2. (a) The temporal evolution of TSI as a function of latitude as computed using the irradiance model based on the distribution of the magnetic concentrations observed with HMI/SDO from 08-Oct-2010 to 05-Apr-2012. Solid lines correspond to orbital planes that are inclined by 30 (blue line), 45 (green line), 60 (red line), and 75° (cyan line) with respect to the solar equatorial plane. (b) A comparison of the TSI observed by SORCE and SOHO and the modeled one. Earth's orbital inclination is shown as the least inclined orbit (dashed line) in Figure 2a. (c) The modeled TSI experienced by a planet or spacecraft at 1 AU from the Sun with inclinations shown in Figure 2a. (d) Evolution of the power blocked by sunspots (blue line), power irradiated by large and small-scale bright features (green and red line, respectively), and the variation of the solar luminosity (black line). These values are averaged over a Carrington Rotation.

(around March and October 2011) are observed in the time series for the power blocked by sunspots. These events are followed by periods of higher power radiated by bright features.

[12] The time-averaged latitudinal profiles of the bright structures (large-scale – blue; small-scale black), sunspot depletion (red line) and the net variation of flux density (green line), which are computed from 08-Oct-2010 to 05-Apr-2012,

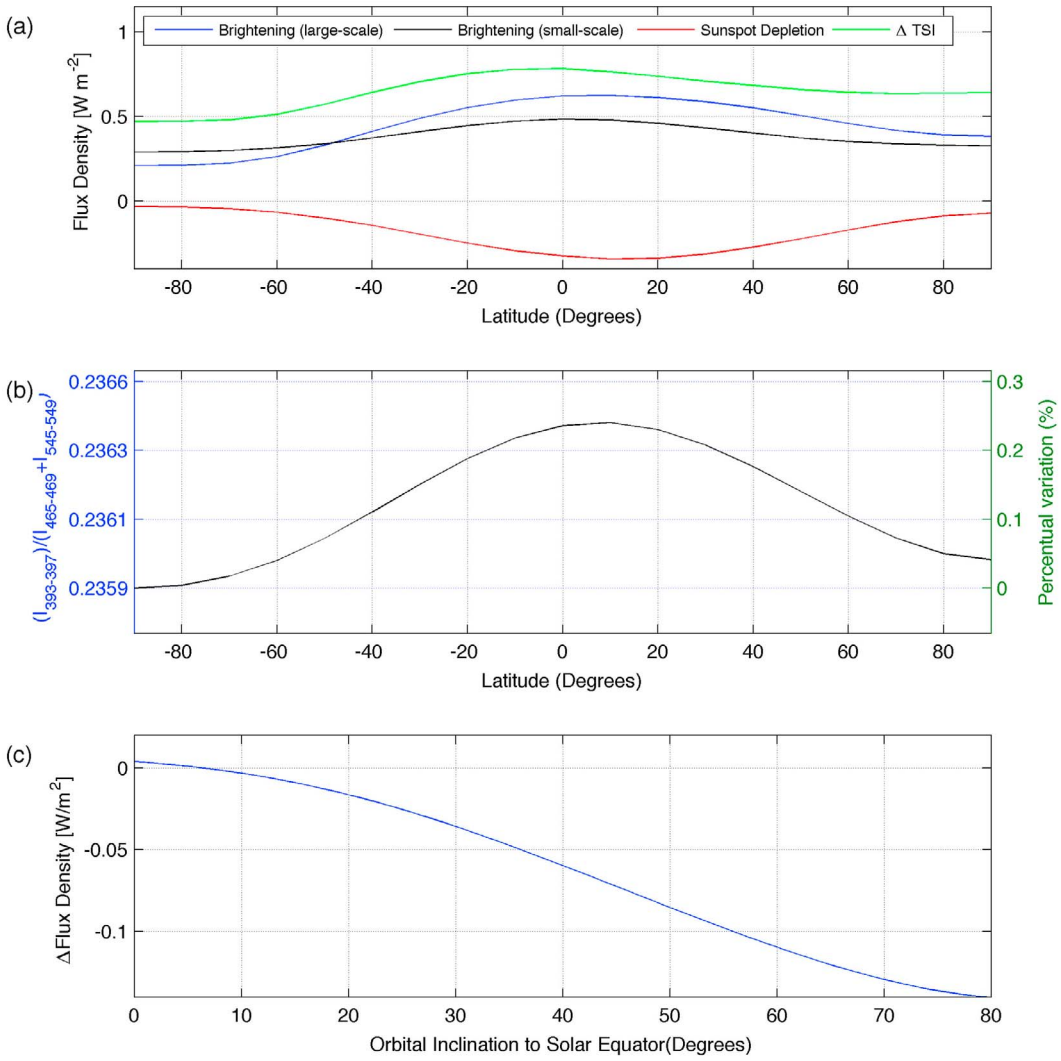

Figure 3. (a) Average latitudinal profiles of the brightening due to large (blue line) and small-scale (black) magnetic concentrations, sunspot depletion (red line) and the net variation of TSI (green line) computed from 08-Oct-2010 to 05-Apr-2012. (b) Estimated ratio between the flux encompassing the Ca II H&K lines (393–397 nm) to the spectral irradiance near the Strömgren b (465–460 nm) and y (545–549 nm) bands. (c) The difference between the TSI observed with inclinations from 0 to 90° and the TSI observed at the Earth's orbit as a function of orbital inclination computed from 08-Oct-2010 to 05-Apr-2012.

are shown if Figure 3a. Note that during the observed period magnetic concentrations were always present on the solar surface. Consequently, the contributions of large and small-scale bright features to the TSI have a minimum value of approximately 0.2 and 0.27 Wm^{-2}, respectively. The asymmetry of the irradiance with respect to the solar equator reflects the predominant emergence of active regions in the Northern hemisphere during the ascending phase of cycle 24, although the contribution from small-scale magnetic concentrations is quasi-symmetrical. For this period, the flux density at the North Pole exceeds the flux density at the South Pole by approximately 0.17 Wm^{-2}. The equatorial brightening of approximately 0.3 Wm^{-2} with respect to the South Pole is caused by the presence of active regions at lower latitudes. While the influence of a sunspot on TSI is greatest when it is at disk center, or at a heliocentric angle of 0°, the influence of faculae/network on TSI increases with center-to-limb angle and projected area, which means that faculae and network affect TSI most when they are at a heliocentric angle of around 55° [*Steiner*, 2005]. Because of these properties, the influence of faculae extends to higher latitudes than the influence of sunspots, suggesting that most of the variability of the irradiance above the poles is due to the evolution of faculae and the network.

[13] The hemispheric asymmetry of the TSI latitudinal profile is not unexpected, as it is common for the Northern and Southern hemisphere to have differences in activity through the solar cycles [*Hathaway*, 2011]. The differences in cycle activity are clearly seen in the sunspot number time series separated by hemispheres (see http://sidc.oma.be/html/wnosuf.html). Additionally, it is also clear for Cycle 24 that the reversal of the Northern polar cap occurs ahead of the Southern polar cap [*Gopalswamy et al.*, 2012].

[14] The latitudinal dependence of the flux density has been proposed to explain why the Sun seems less active than its stellar counterparts [*Knaack et al.*, 2001; *Lockwood et al.*, 2007; *Radick et al.*, 1998; *Schatten*, 1993]. Figure 3b shows the estimated ratio between the flux encompassing the Ca II

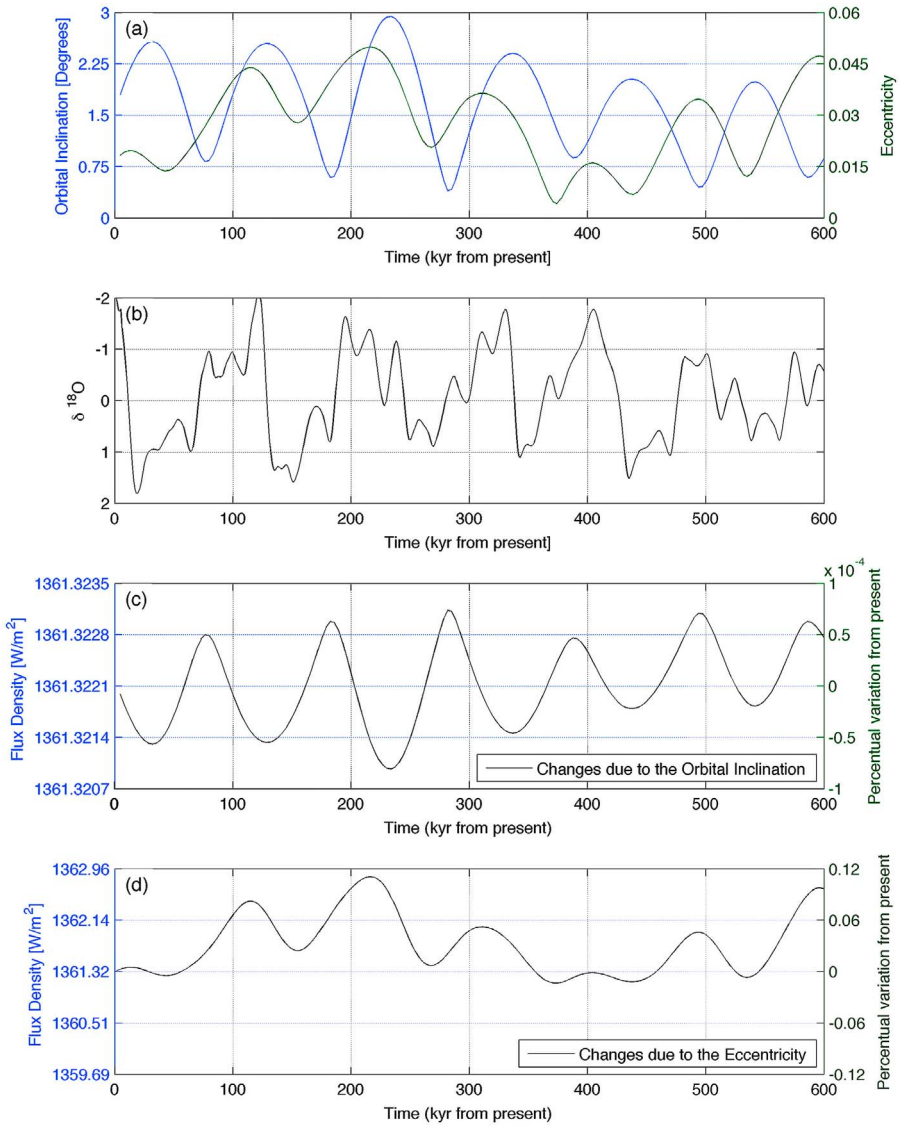

Figure 4. (a) Long term variation of the Earth's orbital inclination with respect to the invariable plane (blue) and the orbital eccentricity (green) as computed by *Varadi et al.* [2003] for 600 kyrs from present. (b) The $\Delta^{18}O$ climate data from SPECMAP that can be considered as a proxy for global temperature of the Earth. (c) The estimated changes of TSI due to orbital inclination, as modeled by using the irradiance model based on HMI data for solar surface features from 08-Oct-2010 to 05-Apr-2012. (d) The estimated changes of TSI due to the orbital eccentricity as computed by *Laskar et al.* [2004].

H&K lines (393–397 nm) to the flux near the Strömgren b (465–460 nm) and y (545–549 nm) bands. The difference between the ratio near the equator and the Southern Pole is estimated to be approximately 0.25%. While the results here do not provide a full picture of the variability of flux density out of the ecliptic through the 11-year activity cycle, the small difference of the flux density between the equator and the poles suggests that it would not be enough to account for the difference between solar activity and its stellar analogues.

[15] To evaluate the impact of changes in Earth's orbital inclination, we used HMI data from 08-Oct-2010 to 05-Apr-2012 as an input to the irradiance model and computed the average difference between TSI at more inclined orbits with respect to the present inclination of the Earth's orbit. Figure 3c shows variations in TSI (flux density) with respect to the present orbit as a function of orbital inclination. Orbits with inclinations lower than the present inclination had slightly higher levels of irradiance. On the other hand, the distribution of magnetic structures led to lower levels of irradiance for more highly inclined orbits.

[16] We stress that this scenario may change during higher activity mainly due to the presence of more magnetic field structures resulting from decaying active regions at higher latitudes.

4. Variations of the TSI Due to Changes of the Orbital Inclination

[17] Although limited by the time period of the HMI/SDO data to the ascending phase of cycle 24, the results presented in the previous section can be used to estimate past variations of the TSI due to changes of the orbital inclination. For this, we assume that the activity belts appeared in the same region that they have been observed since the beginning of

systematic telescopic observations, i.e., between −/+40° of the solar equator [*Hathaway*, 2011].

[18] Figure 4a shows variations of the terrestrial inclination to the invariable plane (blue) and the orbital eccentricity (green) as computed by *Varadi et al.* [2003] for 600 kyr to present. For reference, Figure 4b displays $\Delta^{18}O$ climate data from SPECMAP [*Imbrie et al.*, 1989], considered as a proxy for climate change. As pointed out by *Muller and MacDonald* [1995], the delayed response of ice coverage to the inclination lags approximately 33 kyrs with respect to orbital inclination. We point out, however, that the SPECMAP $\Delta^{18}O$ stack is orbitally tuned using precession and obliquity elements [*Imbrie et al.*, 1989], so phasing of $\Delta^{18}O$ and the Milankovitch cycles (except eccentricity) are not informative.

[19] Using the orbital inclination calculations of *Varadi et al.* [2003], we reconstructed the TSI for the past 600 kyrs in Panel (c) of Figure 4. As discussed above, for large variations of orbital inclination, the TSI changes by up to 0.14 Wm^{-2}. However, variations of the Earth's orbital inclination during the last 600 kyrs were 2.5° or less. In this scenario, the maximum TSI modulation due to orbital inclination is $\sim 3 \times 10^{-3}$ Wm^{-2}. This value is very small, and is lower than the 1-sigma error of 0.05 Wm^{-2} within the model output. By comparison, the maximum annually integrated change related to orbital eccentricity variations is $\sim$1.5 Wm^{-2} (see Figure 4d).

5. Concluding Remarks

[20] To investigate the potential effects of changes in the Earth's orbital inclination on incoming solar irradiance, we estimated changes in solar irradiance as a function of heliographical latitude during the ascending phase of cycle 24. Our approach is based on the principles of physics-based models that have been successfully employed to reconstruct the total and spectral solar irradiance observed by instruments onboard near-Earth space platforms [*Ball et al.*, 2012; *Krivova et al.*, 2003; *Wenzler et al.*, 2006]. Such models, employed for estimating the evolution of irradiance on time scales from days to millennia, are based on the assumption that all changes in the TSI are caused by the evolution of the solar magnetic field. Additionally, our modeling effort relies on the assumption that small-scales structures with scales smaller than we have employed in to compute the flux density are produced by a local surface dynamo [*Vögler and Schüssler*, 2007], and are uniformly distributed over the solar surface, including polar regions, and do not change throughout the 11-year activity cycle.

[21] We found that TSI levels at the North Pole and South Pole during the ascending phase of cycle 24 were significantly different. The difference results from the hemispheric imbalance of magnetic features observed during this period. Most of this activity was observed in the Northern Hemisphere. The TSI asymmetry in the Northern and Southern hemisphere was also observed at midlatitudes, although less pronounced. However, the gradient in TSI between observations from the equator and the poles is not very large, certainly not enough to account for the discrepancy between the activity of the Sun and its stellar analogues, even when accounting for various inclinations of the observer with respect to stellar rotation axes.

[22] We stress that our modeling of the radiation field does not include the latitudinal variations in the thermal structure of the solar convection zone [*Rast et al.*, 2008], which may be needed by models of the solar differential rotation and meridional circulation that best reproduce helioseismic observations [e.g., *Rempel*, 2005].

[23] Based on the latitudinal dependence of solar irradiance, we estimated the variability of the TSI due to changes in orbital inclination. We determined that observers with larger orbital inclinations than the present one would experience a decrease of the TSI up to 0.14 Wm^{-2}. However, changes in the Earth's orbital inclination were only approximately 2.5° during the last 600 kyrs, which resulted in changes in TSI of $\sim 3 \times 10^{-3}$ Wm^{-2}. Therefore, we conclude that while variations in orbital inclinations can cause slight differences in the TSI, these changes are too small to account for the 100 kyr periodicity observed in climate records.

[24] It remains to be seen whether or not our results will be confirmed once data for a longer period of time, and thus not limited to the ascending phase of the cycle, is used.

[25] **Acknowledgments.** We thank the SORCE and SOHO scientific teams for total solar irradiance data and the Joint Science Operations - Science Data Processing (SDP) for SDO/HMI images. The TIM/SORCE data is available at http://lasp.colorado.edu/sorce/data/tsi_data.htm, while the VIRGO/SOHO data is available at http://www.pmodwrc.ch/pmod.php?topic=tsi/virgo/proj_space_virgo#Data. Our work was supported by the European Commission's Seventh Framework Programme (FP7/2007-2013) under grant agreement 261948 (ATMOP Project).

[26] The Editor thanks Margit Haberreiter and an anonymous reviewer for their assistance in evaluating this paper.

References

Ammann, C. M., G. A. Meehl, W. M. Washington, and C. S. Zender (2003), A monthly and latitudinally varying volcanic forcing dataset in simulations of 20th century climate, *Geophys. Res. Lett.*, *30*(12), 1657, doi:10.1029/2003GL016875.

Ball, W. T., Y. C. Unruh, N. A. Krivova, S. Solanki, T. Wenzler, D. J. Mortlock, and A. H. Jaffe (2012), Reconstruction of total solar irradiance 1974–2009, *Astron. Astrophys.*, *541*, A27, doi:10.1051/0004-6361/201118702.

Borrero, J. M., and K. Ichimoto (2011), Magnetic structure of sunspots, *Living Rev. Sol. Phys*, *8*, 4.

Cubasch, U., G. A. Meehl, G. J. Boer, R. J. Stouffer, M. Dix, A. Noda, C. A. Senior, S. Raper, and K. S. Yap (2001), Projections of future climate change, in *Climate Change 2001: The Scientific Basis. Contribution of Working Group I to the Third Assessment Report of the Intergovernmental Panel on Climate Change*, edited by J. T. Houghton et al., pp. 525–582, Cambridge Univ. Press, Cambridge, U. K.

Domingo, V., et al. (2009), Solar surface magnetism and irradiance on time scales from days to the 11-year cycle, *Space Sci. Rev.*, *145*(3), 337–380.

Eddy, J. A. (1976), The Maunder minimum, *Science*, *192*, 1189–1202, doi:10.1126/science.192.4245.1189.

Foukal, P., C. Frohlich, H. Spruit, and T. M. L. Wigley (2006), Variations in solar luminosity and their effect on the Earth's climate, *Nature*, *443*(7108), 161–166, doi:10.1038/nature05072.

Foukal, P., A. Ortiz, and R. Schnerr (2011), Dimming of the 17th century Sun, *Astrophys. J.*, *733*(2), L38, doi:10.1088/2041-8205/733/2/L38.

Fröhlich, C., et al. (1995), VIRGO: Experiment for helioseismology and solar irradiance monitoring, *Sol. Phys.*, *162*, 101–128, doi:10.1007/BF00733428.

Gopalswamy, N., S. Yashiro, P. Mäkelä, G. Michalek, K. Shibasaki, and D. H. Hathaway (2012), Behavior of Solar Cycles 23 and 24 revealed by microwave observations, *Astrophys. J.*, *750*(2), L42, doi:10.1088/2041-8205/750/2/L42.

Hansen, J. E. (2000), The Sun's role in long-term climate change, *Space Sci. Rev.*, *94*(1–2), 349–356, doi:10.1023/A:1026748129347.

Hathaway, D. (2011), A standard law for the equatorward drift of the sunspot zones, *Sol. Phys.*, *273*(1), 221–230, doi:10.1007/s11207-011-9837-z.

Imbrie, J., A. McIntyre, and A. C. Mix (1989), Oceanic response to orbital forcing in the late Quaternary: Observational and experimental strategies, in *Climate and Geosciences, A Challenge for Science and Society in the 21st Century*, edited by S. H. S. A. Berger and J.-C. Duplessy, pp. 121–164, Springer, Berlin, doi:10.1007/978-94-009-2446-8_7.

Knaack, R., M. Fligge, S. K. Solanki, and Y. C. Unruh (2001), The influence of an inclined rotation axis on solar irradiance variations, *Astron. Astrophys.*, *376*(3), 1080–1089, doi:10.1051/0004-6361:20011007.

Kopp, G., and J. L. Lean (2011), A new, lower value of total solar irradiance: Evidence and climate significance, *Geophys. Res. Lett.*, *38*(1), L01706, doi:10.1029/2010GL045777.

Kopp, G., G. Lawrence, and G. Rottman (2005), The Total Irradiance Monitor (TIM): Science results, *Sol. Phys.*, *230*(1–2), 129–139, doi:10.1007/s11207-005-7433-9.

Krivova, N. A., S. K. Solanki, M. Fligge, and Y. C. Unruh (2003), Reconstruction of solar irradiance variations in cycle 23: Is solar surface magnetism the cause?, *Astron. Astrophys.*, *399*(1), L1–L4, doi:10.1051/0004-6361:20030029.

Kurucz, R. (1993), ATLAS9 Stellar Atmosphere Programs and 2 km/s grid, *Kurucz CD-ROM 13*, Smithson. Astrophys. Obs., Cambridge, Mass.

Laskar, J., P. Robutel, F. Joutel, M. Gastineau, A. C. M. Correia, and B. Levrard (2004), A long-term numerical solution for the insolation quantities of the Earth, *Astron. Astrophys.*, *428*(1), 261–285, doi:10.1051/0004-6361:20041335.

Lockwood, G. W., B. A. Skiff, W. H. Gregory, H. Stephen, R. R. Radick, S. L. Baliunas, R. A. Donahue, and W. Soon (2007), Patterns of photometric and chromospheric variation among Sun-like stars: A 20 year perspective, *Astrophys. J. Suppl. Ser.*, *171*(1), 260–303, doi:10.1086/516752.

Muller, R. A., and G. J. MacDonald (1995), Glacial cycles and orbital inclination, *Nature*, *377*(6545), 107–108, doi:10.1038/377107b0.

Radick, R. R., G. W. Lockwood, B. A. Skiff, and S. L. Baliunas (1998), Patterns of variation among Sun-like stars, *Astrophys. J. Suppl. Ser.*, *118*(1), 239–258, doi:10.1086/313135.

Rast, M. P., O. Ada, and W. M. Randle (2008), Latitudinal variation of the solar photospheric intensity, *Astrophys. J.*, *673*(2), 1209, doi:10.1086/524655.

Rempel, M. (2005), Solar differential rotation and meridional flow: The role of a subadiabatic tachocline for the Taylor-Proudman balance, *Astrophys. J.*, *622*(2), 1320–1332, doi:10.1086/428282.

Schatten, K. H. (1993), Heliographic latitude dependence of the Sun's irradiance, *J. Geophys. Res.*, *98*(A11), 18,907–18,910, doi:10.1029/93JA01941.

Schmidt, G. A., et al. (2012), Climate forcing reconstructions for use in PMIP simulations of the last millennium (v1.1), *Geosci. Model Dev.*, *5*(1), 185–191, doi:10.5194/gmd-5-185-2012.

Schnerr, R. S., and H. C. Spruit (2011), The total solar irradiance and small scale magnetic fields, paper presented at Annual Conference, Astron. Soc. of the Pac., Baltimore, Md.

Schou, J., et al (2012), Design and ground calibration of the Helioseismic and Magnetic Imager (HMI) instrument on the Solar Dynamics Observatory (SDO), *Sol. Phys.*, *275*(1–2), 229–259, doi:10.1007/s11207-011-9842-2.

Shapiro, A. I., W. Schmutz, E. Rozanov, M. Schoell, M. Haberreiter, A. V. Shapiro, and S. Nyeki (2011), A new approach to the long-term reconstruction of the solar irradiance leads to large historical solar forcings, *Astron. Astrophys.*, *529*, A67, doi:10.1051/0004-6361/201016173.

Spruit, H. C. (1977), Heat flow near obstacles in the solar convection zone, *Sol. Phys.*, *55*(1), 3–34, doi:10.1007/BF00150871.

Steiner, O. (2005), Radiative properties of magnetic elements, *Astron. Astrophys.*, *430*(2), 691–700, doi:10.1051/0004-6361:20041286.

Steinhilber, F., J. Beer, and C. Fröhlich (2009), Total solar irradiance during the Holocene, *Geophys. Res. Lett.*, *36*, L19704, doi:10.1029/2009GL040142.

Sun, X., Y. Liu, J. Hoeksema, K. Hayashi, and X. Zhao (2011), A new method for polar field interpolation, *Sol. Phys.*, *270*(1), 9–22, doi:10.1007/s11207-011-9751-4.

Unruh, Y. C., S. K. Solanki, and M. Fligge (1999), The spectral dependence of facular contrast and solar irradiance variations, *Astron. Astrophys.*, *345*(2), 635–642.

Varadi, F., B. Runnegar, and M. Ghil (2003), Successive refinements in long-term integrations of planetary orbits, *Astrophys. J.*, *592*(1), 620–630, doi:10.1086/375560.

Vieira, L. E. A., S. K. Solanki, N. A. Krivova, and I. Usoskin (2011), Evolution of the solar irradiance during the Holocene, *Astron. Astrophys.*, *531*, A6, doi:10.1051/0004-6361/201015843.

Vögler, A., and M. Schüssler (2007), A solar surface dynamo, *Astron. Astrophys.*, *465*(3), L43–L46, doi:10.1051/0004-6361:20077253.

Wenzler, T., S. K. Solanki, N. A. Krivova, and C. Frohlich (2006), Reconstruction of solar irradiance variations in cycles 21–23 based on surface magnetic fields, *Astron. Astrophys.*, *460*(2), 583–595, doi:10.1051/0004-6361:20065752.

Willson, R. C., S. Gulkis, M. Janssen, H. S. Hudson, and G. A. Chapman (1981), Observations of solar irradiance variability, *Science*, *211*(4483), 700–702, doi:10.1126/science.211.4483.700.